0026-895X/96/010105-07$3.00/0

MOLECULAR PHARMACOLOGY, 49:105–111 (1996).

Stereoselective and Regioselective Hydration of 7-Methylbenz[c]acridine-5,6-oxide Enantiomers by Rodent and Human Microsomal Epoxide Hydrolases

SARAH J. ROBERTS-THOMSON, MICHAEL E. McMANUS, COLIN C. DUKE, ROBYN AGNEW, and GERALD M. HOLDER

Department of Pharmacy, University of Sydney, Sydney 2006 Australia (S.J.R.-T., C.C.D., R.A., G.M.H.), and Department of Physiology and Pharmacology, University of Queensland, Queensland 4072, Australia (M.E.M.)

Received June 27, 1995; Accepted September 25, 1995

SUMMARY

In the present study, we studied the regioselectivity and stereoselectivity of human microsomal epoxide hydrolase-catalyzed hydration of the enantiomers of the polycyclic aza-aromatic hydrocarbon K-region oxide, 7-methylbenz[c]acridine-5,6-oxide. We used a human microsomal epoxide hydrolase cDNA amplified from a liver cDNA library and expressed in COS-7 cells. Comparisons were made with the activities of rat and HLM preparations. The determination of the apparent Michaelis-Menten kinetic constants revealed that microsomal epoxide hydrolase, regardless of the source, exhibited enantioselectivity, with the 5*S*,6*R*-oxide being the preferred substrate. Regioselectivity of hydration for each stereoisomer was determined. Expressed human microsomal epoxide hydrolase and HLM catalyzed the attack of water predominantly (~96%) at C_5 of the 5*R*,6*S*-oxide, whereas 5*S*,6*R*-oxide was attacked less selectively (~60% at C_5). These results are discussed in the context of available literature on the regioselectivity and stereoselectivity of rat and rabbit microsomal epoxide hydrolase and represents the first examination of human microsomal epoxide hydrolase regarding its regioselectivity and stereoselectivity of hydration.

Epoxides and arene oxides are formed from alkenes and arenes by cytochrome P450-containing monooxygenases. As intermediates of important biological pathways, such as leukotriene A_4 and squalene-2,3-oxide, and metabolites of many xenobiotic compounds, including carbamazepine and aflatoxin B_1, the occurrence of epoxides is widespread (1). Reactive epoxides and arene oxides can bind covalently to cellular constituents, including DNA, RNA, and protein, resulting in mutagenic, carcinogenic, or toxic effects (1). They may also be hydrated by the addition of water catalyzed by mEH (EC 3.3.2.3) to less reactive *trans*-dihydrodiols. The reaction with mEH is thus an important metabolic step in the detoxification of these compounds. However, the dihydrodiols of some polycyclic aromatic hydrocarbons, formed by the action of cytochrome P450 and mEH, can be further metabolized by cytochrome P450 to yield highly reactive and carcinogenic dihydrodiol epoxides.

This study was funded by a National Health and Medical Research Council grant and an Australian Postgraduate Award (S.J.R.-T.).

The stereochemistry of epoxidation and the regioselectivity and enantioselectivity of hydration are important in many activation reactions (2, 3), as illustrated by the activation of BP to its ultimate carcinogen (2). Rodent and human microsomal preparations preferentially form BP-7*R*,8*S*-oxide, which is hydrated by mEH-catalyzed water addition at the nonbenzylic carbon to form exclusively 7*R*,8*R*-dihydrodiol (2, 4, 5). Human microsomal oxidation of this dihydrodiol enantiomer yields predominantly the ultimate carcinogen, anti-7*R*,8*S*-dihydroxy-9*S*,10*R*-epoxy-7,8,9,10-tetrahydrobenzo[a]pyrene, known as diol-epoxide 2 (6), one of two possible stereoisomers derivable from BP-7*R*,8*R*-dihydrodiol. Other examples illustrate the regioselectivity and stereoselectivity of mEH in the hydration of alkene oxides to glycols (7, 8) and of arene oxides to dihydrodiols (9, 10). Except for one study involving HLM (4), all of these studies involve preparations of rabbit or rat liver mEH. The regioselectivity and stereoselectivity of human mEH have not been studied.

We report for the first time a study designed to examine

ABBREVIATIONS: mEH, microsomal epoxide hydrolase; 7MBAC, 7-methylbenz[c]acridine; 7MBAC-5,6-oxide, 7-methylbenz[c]acridine-5,6-oxide; 7MBAC-5,6-DHD, *trans*-5,6-dihydro-5,6-dihydroxy-7-methylbenz[c]acridine; BP, benzo[a]pyrene; HPLC, high performance liquid chromatography; THF, tetrahydrofuran; *Taq* polymerase, *Thermus aquaticus* polymerase; BSA, bovine serum albumin; PB, phenobarbital; PCR, polymerase chain reaction; BP-4,5-oxide, benzo[a]pyrene-4,5-oxide; BP-4,5-DHD, *trans*-4,5-dihydro-4,5-dihydroxy-benzo[a]pyrene; PAR, peak area ratio; *cis*-7MBAC-5,6-DHD, *cis*-5,6-dihydroxy-5,6-dihydro-7-methylbenz[c]acridine; (−)-HCA, (−)-endo-1*S*,4*R*,5,6,7,7-hexachlorobicyclo[2.2.1]-hept-5-ene-2*R*-carboxylic acid; HLM, human liver microsomes.

the regioselectivity and enantioselectivity of hydration of expressed human mEH. In this study, we investigate the hydration of the enantiomers of the aza-aromatic K-region oxide, 7MBAC-5,6-oxide (Fig. 1). In previous work (11), we showed that expressed cytochrome P450 1A1 predominantly formed the 5*S*,6*R*-oxide from 7MBAC, whereas cytochromes P450 1A2 and P450 3A4 produced racemic material. In the current study, we describe the enantiomeric composition of the 5,6-dihydrodiols isolated concurrently with the oxide (11). This is, to our knowledge, the first examination of the stereochemistry of human mEH.

Materials and Methods

Chemicals and enzymes. (−)-HCA, *trans*-7MBAC-5,6-DHD, and racemic 7MBAC-5,6-oxide were available through previous chemical syntheses in our laboratory (12–15). Other materials (and suppliers) were 4-dimethylaminopyridine and *bis*-1,1′-naphthol (Fluka Chemicals, Darmstadt, Germany); restriction enzymes and reagents used in molecular biology (New England Biolabs, Labrador, Queensland, Australia); Dulbecco's modified Eagle's medium (GIBCO-BRL, Melbourne, Australia); NuSerum (Collaborative Research, Bedford, MA); Express ^{35}S protein labeling mix (DuPont, Melbourne, Australia); *Taq* polymerase (Perkin-Elmer Cetus, Frewville, Australia); silica gel (Merck 7736); and BSA (Boehringer Mannheim, Sydney, Australia). Hexane fraction was the BP 68–75° distillate from petroleum spirit. All other chemicals, enzymes and reagents were of HPLC or analytical quality.

Instrumentation. Proton NMR spectra were recorded on a Varian Gemini (300 MHz) spectrometer. Chemical ionization mass spectra were obtained with a Finnigan TSQ-46 mass spectrometer with methane as reagent gas. Circular dichroic spectra of optically active compounds were measured with a JASCO J-500C Spectropolarimeter with a DP-500N data system (Japan Spectroscopic Co. Ltd., Tokyo, Japan). The spectra were recorded over 200–280 nm, and the cell path length was 1 mm. A Beckman System Gold HPLC included a 168 linear diode array spectrophotometric detector that allowed UV spectra to be recorded during peak elution.

Resolution of *cis*-7MBAC-5,6-DHD. *cis*-7MBAC-5,6-DHD was prepared as described (13). Acid chloride of (−)-HCA (654 mg), prepared by refluxing with thionyl chloride (4 ml) for 2 hr (16), was dissolved in THF (4.0 ml) and added to a stirred solution of 4-dimethylaminopyridine (328 mg) and (±)-*cis*-7MBAC-5,6-DHD (200 mg) in THF (4 ml) under nitrogen. After 90 min, the reaction mixture was partitioned between 20% aqueous NaCl and EtOAc. The EtOAc phase was dried (Na_2SO_4), and the solvent was removed under reduced pressure. The diastereoisomeric esters were separated by short column vacuum chromatography (solvent gradient chloroform/hexane fraction, 1:9 to 1:1) (16) to give the less polar diastereoisomer (205 mg, 61%), which was identified as *cis*-5*R*,6*S*-*bis*[endo-1*S*,4*R*,5,6,7,7-hexachlorobicyclo[2.2.1]hept-5-en-2*R*-yl-carbonyloxy]-5,6-dihydro-7-methylbenz[*c*]acridine; CIMS (reagent gas NH_3) m/z (relative intensity) $^{35}Cl/^{37}Cl$ isotope cluster: $^{35}Cl_6{}^{37}Cl_6$ 938 (17), $^{35}Cl_7{}^{37}Cl_5$ 936 (25), $^{35}Cl_8{}^{37}Cl_4$ 934 (45), $^{35}Cl_9{}^{37}Cl_3$ 932 (100), $^{35}Cl_{10}{}^{37}Cl_2$ 930 (89), $^{35}Cl_{11}{}^{37}Cl_1$ 928 (50), and $^{35}Cl_{12}$ 926 (13); ^1H NMR (2 mg/0.7 ml, $CDCl_3$) δ 2.26–2.83 (m, 4H), δ 3.43–3.82 (m, 2H), δ 6.31 (dd, H_5), δ 6.81 (d, H_6), δ 2.82 (s, 7Me), δ 8.68 (d, H_1), δ 8.30 (d, H_{11}), δ 8.35 (dd, H_8), δ 7.81 (m, 2H), δ 7.61 (m, ^3H), and $J_{5,6}$ = 3.1 Hz. UV spectrum in methanol (max in nm [ε]) 268.5 (35,900). The more polar diastereoisomer (188 mg, 56%) was identified as *cis*-5*S*,6*R*-*bis*-[endo-1*S*,4*R*,5,6,7,7-hexachlorobicyclo[2.2.1]hept-5-en-2*R*-yl-carbonyloxy]-5,6-dihydro-7-methylbenz[*c*]acridine; CIMS (reagent gas NH_3) m/z (relative intensity) $^{35}Cl_6{}^{37}C_6$ 938 (12), $^{35}Cl_7{}^{37}Cl_5$ 936 (31), $^{35}Cl_8{}^{37}Cl_4$ 934 (52), $^{35}Cl_9{}^{37}Cl_3$ 932 (71), $^{35}Cl_{10}{}^{37}Cl_2$ 930 (100), $^{35}Cl_{11}{}^{37}Cl_1$ 928 (55), and $^{35}Cl_{12}$ 926 (13); ^1H NMR (2 mg/0.7 ml, $CDCl_3$), δ 2.25–2.9 (m, 4H), δ 3.38–4.00 (m, 2H), δ 6.38 (dd, H_5), δ 6.60 (d, H_6), δ 2.82 (s, 7Me), δ 8.75 (d, H_1), δ 8.28 (d, H_{11}), δ 8.45 (dd, H_8), δ 7.79 (m, 1H), δ 7.61 (m, ^3H), δ 7.4 (m, 1H), and $J_{5,6}$ = 2.9 Hz. UV spectrum in methanol (max in nm [ε]) 268.5 (39,000).

Each diastereoisomer was dissolved in THF (10 ml), and then 10% aqueous sodium hydroxide (1 ml) and methanol (2 ml) were added. After 1 hr, the products were isolated by extraction into ether and washed with water and NaCl, and the ether was dried (Na_2SO_4). Removal of the ether yielded the crude dihydrodiols that were purified by short-column vacuum chromatography (solvent gradient CH_2Cl_2 to 1% ethanol/chloroform) to yield *cis*-7MBAC-5*S*,6*R*-dihydrodiol (45.8 mg), CD spectrum in methanol (M^{-1} cm^{-1}): $\Delta\epsilon_{229}$ −22.54, $\Delta\epsilon_{210}$ 18.95; and *cis*-7MBAC-5*R*,6*S*-dihydrodiol (51.0 mg), CD spectrum in methanol (M^{-1} cm^{-1}): $\Delta\epsilon_{229}$ 26.18, $\Delta\epsilon_{210}$ −21.51, as white solids.

Enantiomers of 7MBAC-5,6-oxide. *cis*-7MBAC-5*R*,6*S*-dihydrodiol (47.6 mg) was suspended in benzene (6 ml) containing trimethylorthoacetate (0.1 ml) and benzoic acid (4 mg). The reaction mixture was distilled at the rate of 1 ml/hr for 3 hr under nitrogen. After cooling to room temperature, anhydrous Na_2CO_3 (25 mg) was added to the reaction mixture, which was then filtered and evaporated to dryness. The residue was dissolved in CH_2Cl_2 (4 ml) and added at 0° to a solution of trimethylsilyl chloride (0.1 ml) and triethylamine (0.01 ml) in CH_2Cl_2 (2 ml). The solvent was evaporated under reduced pressure, and the residue was dissolved in THF (10 ml), which was then added slowly to dry sodium methoxide (140 mg) in THF (5 ml) at −78° under nitrogen. The reaction was allowed to warm to 4° and stirred for 30 min. The crude product was extracted into EtOAc and washed with water, and the EtOAc was dried over $MgSO_4$. After removal of solvent under reduced pressure, the crude product was purified by short-column vacuum chromatography (solvent gradient CH_2Cl_2/hexane fraction 1:9 to CH_2Cl_2/hexane fraction 1:1) to yield pure 7MBAC-5*R*,6*S*-oxide as a white crystalline solid (22.8 mg, 51.2%); CIMS m/z (relative intensity): 300 (M+41, 8), 288 (M+29, 21), 260 (M+1, 87), 244 (100). 7MBAC-5*S*,6*R*-oxide was formed in the same way from *cis*-7MBAC-5*S*,6*R*-dihydrodiol (48.3 mg) to yield the oxide as a white crystalline solid (24.6 mg, 56%); CIMS m/z was identical with 7MBAC-5*R*,6*S*-oxide.

Base-catalyzed methanolysis of 7-methylbenz[*c*]acridine-5,6-oxide enantiomers. 7MBAC-5*R*,6*S*-oxide (500 μg) was added to a solution of sodium methoxide (30 mg sodium in 4 ml methanol) and stirred under nitrogen. The reaction was heated at 60° and shown by thin layer chromatography to be complete. The methanol was removed under reduced pressure, and the products were partitioned between EtOAc and 20% aqueous NaCl. The EtOAc phase was dried over Na_2SO_4 and filtered, and solvent was removed under reduced pressure. Chiral stationary-phase HPLC on a Pirkle (*R*)-3,5-(dinitrobenzoyl)phenylglycine ionically bound to 3-aminopropyl silanized silica (Regis Chemical Co., Morton Grove, IL) with 3.3% EtOH and 1.7% acetonitrile in hexane at 1.0 ml/min was used to separate the products (17) and afforded 5,6-dihydro-6*S*-hydroxy-5*S*-methoxy-7MBAC (28.7 min) and 5,6-dihydro-5*R*-hydroxy-6*R*-methoxy-7MBAC (31.4 min). The same procedure was repeated on 7MBAC-5*S*,6*R*-oxide (500 μg) and afforded 5,6-dihydro-6*R*-hydroxy-5*R*-methoxy-7MBAC (26.6 min) and 5,6-dihydro-5*S*-hydroxy-6*S*-methoxy-7MBAC (32.8 min). The chromatographic peaks at 26.6 and 28.7 min were well resolved (resolution value 2.0) and allowed accurate estimations of the optical purities (enantiomeric excess) as 98.4% for 7MBAC-5*S*,6*R*-oxide and 99.0% for 7MBAC-5*R*,6*S*-oxide.

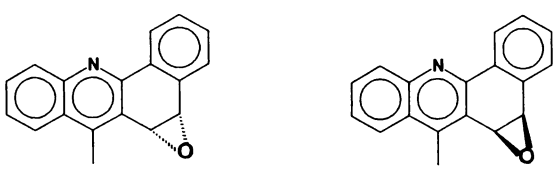

7MBAC-5S,6R-oxide 7MBAC-5R,6S-oxide

Fig. 1. Enantiomeric 7MBAC-5,6-oxides.

Human and rat liver microsomes. HLM were available from previous work (18). Sprague-Dawley rat liver microsomes were prepared as previously described (15, 19) after pretreatment of the animals with intraperitoneal doses of PB in saline (60, 80, and 100 mg/kg daily for 3 consecutive days). Protein concentrations were determined according to the method of Lowry *et al.* (20).

Cloning of human mEH cDNA using PCR. Primers were designed using a previously published sequence for the human mEH cDNA (21) and adapted to contain unique restriction sites. The forward primer was 5′-GTA GAT CTA GGG TGA GAA CGT GGA GC-3′ and the reversed primer was 5′-CGT AAG CTT TCA AAG CCA TGT TGC TTA CC-3′. Template DNA was isolated from a human liver λgt11 cDNA library, designated Pa86 (obtained from Dr. F. J. Gonzalez, Laboratory of Molecular Carcinogenesis, National Institutes of Health, Bethesda, MD), and used at a concentration of 20 ng/100 μl. DNA amplification was carried out with a Perkin-Elmer Cetus DNA thermal cycler in a 100-μl volume containing 16.6 mM $(NH_4)_2SO_4$, 67.0 mM Tris·HCl, pH 8.8, 10.0 mM 2-mercaptoethanol, 2.0 mM $MgCl_2$, 200 μg/ml gelatin, 0.1 mM of each deoxynucleoside triphosphate, 0.125 μM of each primer, and 0.16 units/100 μl of *Taq* polymerase. Forty-five cycles of amplification were performed (94° for 1 min, 50° for 1 min, and 72° for 3 min), and 10% of the product was analyzed on a 1% agarose gel.

Subcloning mEH cDNA into $pCMV_5$ and pBS. After removal of *Taq* polymerase, the remaining PCR mix was purified by electrophoresis on a 1.5% low melting point agarose gel followed by precipitation of the DNA by ethanol. The PCR products were then cut with *Bgl*II and *Hin*dIII and subcloned into $pCMV_5$. The cDNAs were expressed and their activities were determined by incubation with BP-4,5-oxide. The mEH insert of the most active clone was also subcloned into the *Bam*HI and *Hin*dIII sites of pBS (Stratagene, La Jolla, CA), and the nucleotide sequence was determined using a T7 sequence kit (United States Biochemical Corporation, Cleveland, OH).

Expression of mEH cDNA in COS-7 cells. The cDNA for mEH was expressed as previously described (11, 22), and expression was detected by immunoblotting (18) using rabbit anti-rat microsomal epoxide hydrolase antiserum.

Metabolism of BP-4,5-oxide by expressed mEH. Incubations (0.5 ml) contained COS cell lysate (0.2 mg), BSA (0.4 mg), and BP-4,5-oxide (25 μM added to 10 μl acetonitrile) in 0.1 M Tris·HCL buffer, pH 8.7. Control incubations consisted of COS cells transfected with expression vector alone. After incubation at 37° for 30 min, the reaction was stopped by the addition of EtOAc (1 ml) containing the internal standard (9,10-phenanthrenequinone, 0.8 μg). After an additional EtOAc extraction (1 ml), the organic layers were pooled, the EtOAc was removed under vacuum, and the residue was redissolved in acetonitrile (80 μl) for HPLC.

Analysis of BP-4,5-oxide metabolites by HPLC. BP-4,5-oxide was separated from BP-4,5-DHD and the internal standard by reversed-phase HPLC with a 5-μm Hibar RP-8 column (250 × 4 mm inside diameter, Merck, Darmstadt, Germany) using UV detection at 271 nm, a flow rate of 1.0 ml/min, and a column temperature of 40°. Isocratic elution with 10% methanol/sodium phosphate buffer (5 mM, pH 6.8) for 14 min was followed by a rapid linear change over 1 min to 100% methanol, and the unchanged oxide emerged at a retention time of 15.2 min. The retention times of BP-4,5-DHD and the internal standard were 9.8 and 4.6 min, respectively, and quantitative data were obtained from a standard curve using PARs.

Metabolism of 7MBAC-5,6-oxide by mEH. Incubations (1.0 ml) contained protein, substrate (0.3–60 μM, added in 5 μl acetonitrile), and BSA (0.4 mg) in Tris·HCl buffer (0.1 M, pH 8.7). After incubation at 37°, the reaction was stopped by rapid cooling in ice, and EtOAc (2 ml) containing the internal standard (bis-1,1′-naphthol, 15 μg) was added. The organic layer was removed and then combined with a second extraction with EtOAc (2 ml). The solvent was removed under vacuum, and the residue was dissolved in acetonitrile (80 μl) for HPLC. Blanks contained all components except protein and afforded no dihydrodiols. All determinations were carried out in triplicate. For 7MBAC-5*S*,6*R*-oxide, the protein concentration and incubation times were 5 μg/ml and 10 min, 3 μg/ml and 4 min, and 2–5 μg/ml and 4–10 min for COS cell-expressed human mEH and rat and human liver mEH, respectively. For 7MBAC-5*R*,6*S*-oxide, values were 60 μg/ml and 10 min, 0.3 mg/ml and 15 min, and 20–25 μg/ml and 5–15 min, respectively. For all preparations, product formation was linear with incubation time and protein concentration and no more than 10–15% of the substrate was consumed. Kinetic parameters were determined using the computer software PCNONLIN Version 4.2 (Scientific Consulting, Apex, NC).

Analysis of 7MBAC-5,6-oxide metabolites by HPLC. 7MBAC-5,6-oxide, the dihydrodiol and internal standard were separated on reversed-phase HPLC with a 5-μm Hibar RP-8 column (250 × 4 mm inside diameter, Merck, Darmstadt, Germany), a column temperature of 40°, UV detection at 264 nm, and a flow rate of 0.8 ml/min. After 6 min of isocratic elution with 52% methanol in sodium phosphate buffer (5 mM, pH 6.8), the methanol was ramped linearly to 68% followed by a second isocratic period of 19 min. Retention times were 20.6, 6.7, and 16.1 min for the oxide, dihydrodiol, and internal standard, respectively, and quantitative data were obtained from a standard curve using PARs.

Regioselectivity of 7MBAC-5,6-DHD formation. For 7MBAC-5*S*,6*R*-oxide, the EtOAc extracts from three 20-min incubations containing 26 μM substrate (expressed mEH) or from three 15-min incubations with 30 μM substrate (human microsomes) were pooled. For expressed mEH and HLM, the EtOAc extracts were pooled from six incubations for 30-min (8 μM substrate) or three 15-min incubations (30 μM substrate) with 7MBAC-5*R*,6*S*-oxide, respectively. The dihydrodiol was separated from unchanged oxide by HPLC with the conditions described above, and the 7MBAC-5,6-DHD fraction was collected. It was then evaporated to dryness and dried over phosphorus pentoxide for at least 17 hr before conversion to its bis-(+)-(1*S*,2*R*,4*R*)-endo-1,4,5,6,7,7-hexachlorobicyclo[2.2.1]-hept-5-ene-2-carboxylic acid esters (11). After separation of the diastereoisomeric esters on normal-phase HPLC as described (11), the relative amount and absolute configuration of each enantiomer were determined from previous chromatographic behavior and peak area measurements.

Results

Synthesis and resolution of 7MBAC-5,6-oxide enantiomers. *cis*-7MBAC-5,6-dihydrodiol was resolved as its bis-(−)-HCA esters (12, 16), and these were converted to the enantiomers of 7MBAC-5,6-oxide via the 1,3-dioxolane and halohydrin acetate (23). The absolute configurations of the *cis*-dihydrodiols were assigned from their CD spectra by comparison with those of their *trans*-isomers (17). The 6-hydroxy groups of the *cis*-isomers were expected to adopt the quasiaxial conformation to avoid steric interaction with the 7-methyl group, and the helicity of the 2-phenylquinoline was predictable as M (left-handed) for the 5*S*,6*R*-isomer and as P (right-handed) for the 5*R*,6*S*-isomer. With *trans*-7MBAC-5,6-DHD enantiomers, the conformation of the hydroxyl groups is quasidiaxial, and the CD spectrum of the 5*R*,6*R*-isomer displayed strong Cotton effects at 243 nm (negative) and 214 nm (positive). The *cis*-5,6-dihydrodiol enantiomer, which showed such strong negative and positive Cotton effects at 237 and 208 nm, was assigned the 5*S*,6*R* configuration (Fig. 2), and its enantiomer, which showed Cotton effects with reversed signs, was assigned the opposite 5*R*,6*S* configuration. The epoxides derived from the *cis*-dihydrodiols were assigned the same configuration as their diol precursors (23), and these assignments were confirmed by treatment of the epoxides with sodium methoxide and chromatographic com-

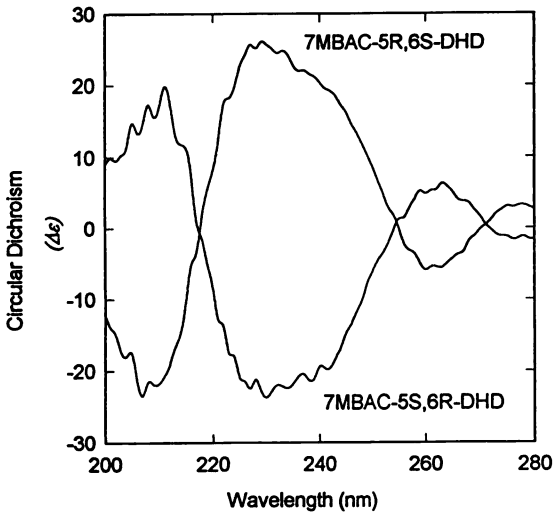

Fig. 2. The CD spectra in MeOH of the enantiomers of *cis*-7MBAC-5,6-DHD.

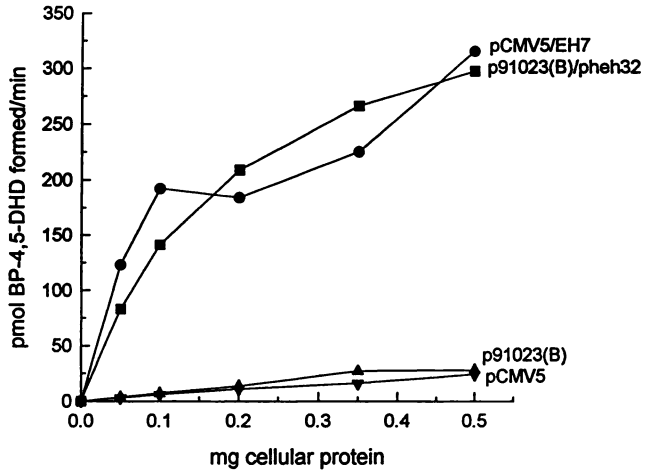

Fig. 4. The capacity of mEH clones to metabolize BP-4,5-oxide to its dihydrodiol. COS cell lysate (0.2 mg) was added to BP-4,5-DHD (25 μM) as described in Materials and Methods. Separation of remaining oxide from dihydrodiol was achieved by reversed-phase HPLC, and quantification was by comparison with a standard curve using PARs. *Data points*, mean of two determinations.

parison of the 5-hydroxy-6-methoxy and 6-hydroxy-5-methoxy products with those characterized previously (17).

Cloning and expression of human mEH. With specific oligonucleotide primers, designed against the human mEH cloned by Skoda *et al.* (21), PCR was used to amplify a mEH cDNA from a human liver λgt11 library. The mEH cDNA used in these studies (EH7) had a deduced amino acid sequence identical to that published by Skoda *et al.* (21). After subcloning into the $pCMV_5$ vector, the EH7 cDNA was expressed in COS-7 cells and gave a protein band on immunoblots that was identical in molecular weight to that observed in HLM, control, and PB-induced rat liver (Fig. 3). No immunodetectable band was seen in COS cells transfected with vector alone. While the expression studies were in progress, Prof. Urs Meyer kindly supplied us with the p91023(B)/pheh32 construct (21), a human mEH cDNA, which when expressed in COS cells produced an immunodetectable band of identical molecular weight to the $pCMV_5$/EH7 construct (Fig. 3). The expression of both $pCMV_5$/EH7 and p91023(B)/pheh32 in COS cells gave proteins that converted BP-4,5-oxide to BP-4,5-DHD at similar rates (Fig. 4). It was observed that in COS cells transfected with either the $pCMV_5$ or p91023(B) plasmid only, a background level of activity for the conversion of BP-4,5-oxide to its dihydrodiol of ~50 pmol/mg cell lysate/min was detectable. This indicates that COS cells do possess some basal mEH activity. For all subsequent experiments, the $pCMV_5$/EH7 construct was used to transfect COS cells to produce recombinant human mEH.

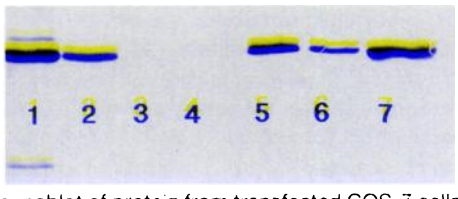

Fig. 3. Immunoblot of protein from transfected COS-7 cells with rabbit anti-rat microsomal epoxide hydrolase antibody. *Lane 1*; 10 μg of total COS cell protein from $pCMV_5$/EH7 transfected COS-7 cells; *lane 2*; 25 μg total cell protein from p91023(B)/pheh32 transfected COS-7 cells; *lane 3*; 10 μg total cell protein from $pCMV_5$ transfected COS-7 cells; *lane 4*; 10 μg total cell protein from p91023(B) transfected cells; *lane 5*; 1 μg of microsomal protein from PB-induced rat liver microsomes; *lane 6*; 1 μg of microsomal protein from control rat liver microsomes; and *lane 7*; 25 μg of microsomal protein from human liver.

Hydration of 7MBAC-oxide enantiomers. To characterize the ability of recombinant human mEH, HLM, and PB-induced rat liver microsomes to hydrate the enantiomers of 7MBAC-5,6-oxide, optimal reaction conditions were first established with respect to protein concentration and time. In general, each source of mEH gave reaction rates with respect to the hydration of 5*S*,6*R*-oxide and 5*R*,6*S*-oxide that were linear with protein concentration up to 0.1 and 0.7 mg/ml, respectively, and over an incubation time of 20 min. The maximum rate of metabolism was greater for the 5*S*,6*R*-enantiomer for all three sources of mEH (Table 1). For example, for HLM, the mean V_{max} for the metabolism of 7MBAC-5*S*,6*R*-oxide to its dihydrodiol was 38.34 ± 20.47 pmol/mg protein/min (mean ± standard deviation for four determinations) compared with a V_{max} of 5.86 ± 2.06 pmol/mg protein/min (mean ± standard deviation for four determinations) for the conversion of 7MBAC-5*R*,6*S*-oxide to its dihydrodiol. This ~7-fold difference in catalytic activity of HLM for the 5*S*,6*R*-oxide compared with its 5*R*,6*S*-isomer was also reflected by the recombinant human mEH (Table 1). Likewise, for PB-induced rat liver microsomes, the 5*S*,6*R*-oxide was hydrated at a greater maximum rate than the 5*R*,6*S*-oxide but with a difference in catalytic activity of 100-fold.

The mean apparent K_m for the hydration of 7MBAC-5*S*,6*R*-oxide in HLM was 2.89 ± 1.13 (mean ± standard deviation for four determinations). This was significantly less ($p < 0.01$) than the mean apparent K_m calculated for the same human microsomes for the 5*R*,6*S*-oxide enantiomer (8.34 ± 2.42; mean ± standard deviation for four determinations). Similarly, PB-induced rat liver microsomes had a smaller apparent K_m for the hydration of the 5*S*,6*R*-oxide than for the hydration of its isomer. There was no significant difference ($p > 0.05$) between the apparent K_m values for the hydration of each oxide enantiomer by recombinant human mEH. The ratio V_{max}/K_m, representing the substrate reactivity (10), was higher for the 5*S*,6*R*-oxide than for the 5*R*,6*S*-oxide for

TABLE 1

Kinetic constants for the hydration of 7MBAC-5,6-oxide enantiomers by mEH

After incubation at 37°, rates of reaction were determined by reversed-phase HPLC as described in Materials and Methods.

	K_m[a]	V_{max}[b]	V_{max}/K_m
	μM	nmol/mg/min	min^{-1}/mg/ml
7MBAC-5S,6R-oxide			
Expressed human mEH	7.89 ± 1.20	23.62 ± 1.36	3.0 ± 0.6
PB rat liver microsomes	1.98 ± 0.3	48.6 ± 1.83	24.5 ± 4.6
HLM11	1.99 ± 0.31	67.41 ± 2.69	34.0 ± 6.6
HLM19	4.05 ± 0.68	37.34 ± 2.11	9.2 ± 2.1
HLM21	3.66 ± 0.84	21.41 ± 1.53	5.8 ± 1.8
HLM14	1.84 ± 0.15	27.20 ± 0.59	14.8 ± 1.5
7MBAC-5R,6S-oxide			
Expressed human mEH	5.89 ± 1.89	3.31 ± 0.37	0.56 ± 0.24
PB rat liver microsomes	8.92 ± 1.58	0.49 ± 0.03	0.05 ± 0.01
HLM11	7.33 ± 1.38	8.73 ± 0.60	1.19 ± 0.31
HLM19	6.00 ± 0.84	5.96 ± 0.30	0.99 ± 0.19
HLM21	11.66 ± 1.14	4.53 ± 0.20	0.39 ± 0.06
HLM14	8.35 ± 1.19	4.22 ± 0.24	0.51 ± 0.10

[a] Results are expressed as the mean ± the standard error of the fit from three experiments as determined by the program PCNONLIN Version 4.2.

[b] Results are expressed per mg of protein with no standardization for enzyme content.

each mEH source (Table 1). Thus, for all preparations, 7MBAC-5*S*,6*R*-oxide was more reactive in its conversion to dihydrodiol than its 5*R*,6*S*-isomer.

The regioselectivity of water attack for each enantiomer was probed by separately converting each oxide isomer to its enantiomeric dihydrodiol metabolites. After separation of the remaining substrate from the dihydrodiol by reversed-phase HPLC, the dihydrodiol fraction was collected and then converted to its (+)-HCA esters. Normal-phase HPLC was used to separate the diastereoisomeric esters. The poorer substrate was attacked by water almost exclusively at the 5*R*-position, whereas hydration of the 5*S*,6*R*-oxide occurred far less selectively, with attack again favoring the 5-position (Fig. 5). Identical results were obtained with one HLM sample and expressed human mEH.

Discussion

In this report, we examine for the first time the regioselectivity and enantioselectivity of hydration of expressed human mEH and compare it with that of rat and human microsomal preparations. The cDNA for human mEH was amplified using PCR, and its activity toward BP-4,5-oxide was examined. Comparison with pheh32, the clone of Skoda *et al.* (21), showed that both clones had similar activity (Fig. 4). Subsequent determination of the cDNA amino acid sequence of EH7 showed it to be identical to that of pheh32.

The determination of mEH catalytic activity for BP-4,5-oxide showed that cells transfected with the two vectors $pCMV_5$ and p91023(B) produced low amounts of BP-4,5-DHD. This was unexpected because the COS cell line was reported to be free of endogenous mEH (21) and showed the absence of detectable mEH protein by immunoblotting (Fig. 3, *lanes 3 and 4*). The current observations of low mEH activity have also been seen in a recent study with COS-1 cells (24).

Six distinct full-length human mEH cDNA sequences have been cloned (21, 24, 25). The deduced protein sequences of these clones differ by <2% in amino acid content with variation occurring at two residues, amino acids 113 and 139 (24). The human mEH sequences containing Tyr^{113} and His^{139} have been tentatively identified as the most frequently occurring alleles in a study consisting mainly of DNA from a white population (24). This study showed that different combinations of amino acid residues at these positions in mEH protein directly influence enzymatic activity, possibly by affecting protein stability. EH7 has Tyr^{113} and His^{139} and therefore is likely to be the most frequently occurring allele in the white population. This clone was used to study the enantioselectivity and regioselectivity of the hydration of the resolved enantiomers of 7MBAC-5,6-oxide, a K-region arene oxide.

Hydration of 7MBAC-5,6-oxide enantiomers occurred stereoselectively with one enantiomer, with the 5*S*,6*R*-isomer being the preferred substrate. Differences observed in the value of apparent K_m for different preparations of mEH may be a direct result of the microenvironment of the enzyme or suggests different alleles of mEH where base substitution has altered the affinity of the substrate binding. Hydration was regioselective with predominant attack occurring at the 5-position of both enantiomers, the ratio of C5 attack to C6 attack being 23:1 for the 5*R*,6*S*-enantiomer (poorer substrate) and ~6:4 for the 5*S*,6*R*-enantiomer for both HLM and expressed mEH (Table 2).

With rodent and rabbit preparations, enantioselectivity of hydration of aryl-substituted aliphatic oxides has been observed for styrene oxide (7), *p*-nitrostyrene oxide (26), 1-phenylpropene oxides (8), and *cis*-*p*-chlorostilbene oxide (27).

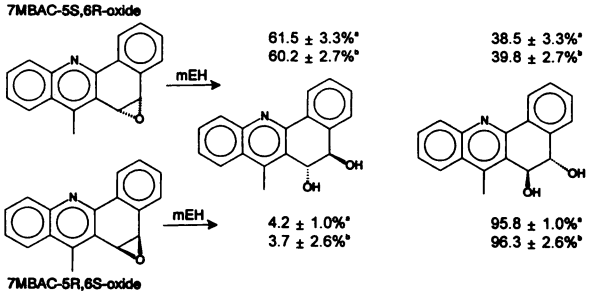

Fig. 5. Schematic representation of the hydration of optically pure 7MBAC-5,6-oxide enantiomers by expressed human mEH and an HLM preparation (HLM21). Results are shown as mean ± standard deviation from three determinations.

TABLE 2

Calculated and experimentally determined ratio of 5*R*,6*R*- to 5*S*,6*S*-enantiomers of 7MBAC-5,6-dihydrodiol

Ratio of 5*R*,6*R*- to 5*S*,6*S*-enantiomers of 7MBAC-5,6-dihydrodiol		
Human cytochrome P450	Calculated[a]	Experimental[b]
1A1	45:55	49:51
1A2	33:67	33:67
3A4	31:69	46:54

[a] Values calculated from the results presented in this study on the regioselectivity of expressed human mEH hydration and the optical purities of the expressed human cytochrome P450 metabolically formed oxides (11).

[b] Experimental values obtained from the dihydrodiol concurrently formed with the oxide by expressed human cytochrome P450 and basal epoxide hydrolase activity of the COS-7 cells (11).

Similar observations have been made for some monosubstituted aliphatic epoxides (28), 1,1-disubstituted oxides (29), cyclic aliphatic oxides (30), aromatic non-K-region oxides (9, 31), and K-region oxides. K-region BP-4*S*,5*R*-oxide (9), benz[a]anthracene-5*S*,6*R*-oxide (9), and dibenz[a,h]anthracene-5*S*,6*R*-oxide (32) have greater rates of hydration than their respective *R*,*S*-isomers. The behavior of the 7MBAC-5,6-oxide enantiomers in this study is analogous to these compounds rather than chrysene-5,6-oxide (33), for which the 5*R*,6*S*-enantiomer is hydrated 6-fold faster than its stereoisomer.

Regioselectivity is evident in the hydration of oxides that are symmetrical, such as *cis*-stilbene oxide (27), phenanthrene-9,10-oxide, pyrene-4,5-oxide, and benzo[e]pyrene-4,5-oxide (34), when water attack occurred predominantly on the oxirane carbon with the *S* configuration. With non-K-region arene oxides such as BP-7,8-oxide, attack occurs preferentially on the non-benzylic oxirane carbon regardless of its configuration, whereas with K-region oxides, the preferred position of attack cannot be defined based on both the substrate and absolute configuration.

Results of the present study show that the K-region 7MBAC-5,6-oxides were attacked predominantly at C_5, with a higher regioselectivity (~96%) seen for the less reactive *R*,*S*-isomer (Fig. 5). This situation is quite unlike those of BP-4,5-oxide and benz[a]anthracene-5,6-oxide, in which the faster reacting enantiomers, 4*S*,5*R* and 5*S*,6*R* configuration, respectively, are attacked almost exclusively at the carbon with the *S* configuration. The less reactive enantiomer of BP-4,5-oxide is also attacked preferentially at the *S*-carbon atom, whereas that of benz[a]anthracene is attacked with almost equal facility at the two positions (9). Dibenz[a,h]anthracene-5,6-oxide enantiomers are also preferentially attacked at the 5-position regardless of its absolute configuration (32). These situations are distinct from that of chrysene, in which attack of water occurs preferentially on the 6-position in the faster reacting 5*R*,6*S*-oxide (33). For methylated benz[a]anthracenes, 12-methylbenz[a]anthracene, and 7,12-dimethylbenz[a]anthracene, attack occurs predominantly on C_6 of the 5*S*,6*R*-oxides to afford the *S*,*S*-dihydrodiols (5). Thus, greatest similarities between the behaviors of the 7MBAC-5,6-oxide enantiomers are seen with benz[a]anthracene and dibenz[a,h]anthracene K-region oxides.

The enantiomeric composition of 7MBAC-5,6-oxide formed catalytically by expressed human cytochromes P450 from the parent hydrocarbon 7MBAC has been previously determined in this laboratory (11). Cytochromes P450 1A2 and P450 3A4 produced essentially racemic oxide, whereas that formed by cytochrome P450 1A1 was predominantly of 5*R*,6*S* configuration (29.6%). Based on the regioselectivity of mEH hydration of the oxide enantiomers (shown in Fig. 5) and the optical purities of metabolically formed oxide previously determined (11), the expected enantiomeric composition of the product dihydrodiol was calculated and compared with that determined in the 5,6-dihydrodiol formed concurrently with oxide by expressed cytochrome P450s (Table 2). The agreement found is excellent in two cases and fair in the third and was obtained in the metabolic experiments with nonsaturating levels of oxides formed biosynthetically with the basal epoxide hydrolase activity of COS cells. This implies that the regioselectivity and stereoselectivity of hydration of 7MBAC K-region oxides by basal mEH of the COS cells are the same as those of human mEH. The low activity of COS cells transfected with vector alone toward BP-4,5-oxide indicated that activities toward 7MBAC-5,6-oxides were too low to allow the determination of regioselectivity and stereoselectivity.

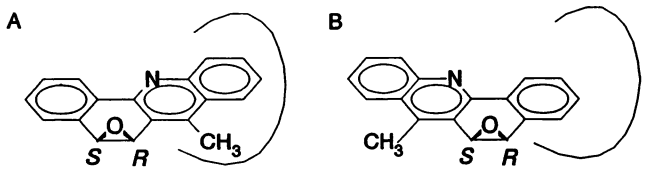

Fig. 6. Illustration of the fit of 7MBAC-5,6-oxide enantiomers into the proposed model. A, 7MBAC-5*S*,6*R*-oxide. B, 7MBAC-5*R*,6*S*-oxide.

The entire human mEH gene has been cloned and sequenced (35), and pivotal work has described the catalytic mechanism and structural organization of this enzyme (36–39). Comparison of the amino acid sequence similarities between species show a high degree of conservation of this enzyme with human mEH, sharing 80% and 84% similarity with rabbit and rat mEH, respectively (21). A model to account for the enantioselectivity of rodent and rabbit mEH has been proposed in which the larger of two aryl groups or a large alkyl substituent binds to a hydrophobic pocket situated to the right and rear of the oxirane function in the preferred enantiomer (9, 40). This was based on the behavior of the hydration of 4-*tert*-butyl-1,2-epoxycyclohexanes, BP-4,5- and BP-7,8-oxides, and benz[a]anthracene-5,6-oxide. With other substrates, the hydrophobic pocket was extended slightly to the left of the oxirane ring (10). 7MBAC-5*S*,6*R*-oxide, the preferred substrate, fits the model (Fig. 6A) better than its enantiomer (Fig. 6B). The regioselectivity of hydration of K-region oxides has been summarized by Yang (5). The *S*,*R*-epoxides derived from planar polycyclic aromatic hydrocarbons are hydrated at the *S*-center to form K-region dihydrodiols enriched in the *R*,*R*-enantiomer. Nonplanar polycyclic aromatic hydrocarbon *S*,*R*-oxides are, in contrast, hydrated at their *R*-centers to form *S*,*S*-dihydrodiols. No rule to predict the behavior of mEH toward the *R*,*S*-oxides of planar and nonplanar hydrocarbons was proposed. The regioselectivity of water attack on the preferred substrate 7MBAC-5S,6R-oxide is consistent with these observations. More extensive studies are warranted to elaborate on the requirements of the human enzyme, its active site, and the modalities of binding.

Acknowledgments

The mEH clone pheh32 was kindly provided by Prof. U. A. Meyer, Department of Pharmacology, Biocenter, University of Basel, Switzerland. The rabbit anti-rat mEH antiserum was the gift of Prof. F. Oesch and Dr. S. Elsberg, Institute of Toxicology, University of Mainz, Germany. The $pCMV_5$ vector was made available by Prof. M. F. Stinski, Department of Microbiology, College of Medicine, University of Iowa, Ames, Iowa. These gifts are gratefully acknowledged. Nucleotide sequencing was carried out by Marjorie Liu from The Garvin Institute of Medical Research, Darlinghurst, N.S.W., Australia. Thanks are due to Dr. Iqbal Ramzan for his helpful discussions.

References

1. Wixtrom, R. N., and Hammock, B. Membrane-bound and soluble-fraction epoxide hydrolases, in *Biochemical Pharmacology and Toxicology. Methodological Aspects of Drug Metabolizing Enzymes* (D. Zakim and D. A. Vessey, eds.). Vol. 1. John Wiley & Sons, New York, 1–95 (1985).
2. Thakker, D. R., H. Yagi, W. Levin, A. W. Wood, A. H. Conney, and D. M. Jerina. Polycyclic aromatic hydrocarbons: metabolic activation to ultimate

carcinogens, in *Bioactivation of Foreign Compounds* (M. W. Anders, ed.). Academic Press, Orlando, FL, 177–242 (1985).
3. Armstrong, R. N. Enzyme-catalyzed detoxication reactions: mechanisms and stereochemistry. *CRC Crit. Rev. Biochem.* **22**:39–88 (1987).
4. Hall, M., L. M. Forrester, D. K. Parker, P. L. Grover, and C. R. Wolf. Relative contribution of various forms of cytochrome P450 to the metabolism of benzo[a]pyrene by human liver microsomes. *Carcinogenesis* **10**: 1815–1821 (1989).
5. Yang, S. K. Stereoselectivity of cytochrome P-450 isozymes and epoxide hydrolase in the metabolism of polycyclic aromatic hydrocarbons. *Biochem. Pharmacol.* **37**:61–70 (1988).
6. Scharping, C. E., M. E. McManus, and G. M. Holder. NADPH-supported and arachidonic acid-supported metabolism of the enantiomers of *trans*-7,8-dihydrobenzo[a]pyrene-7,8-diol by human liver microsomal samples. *Carcinogenesis* **13**:1199–1207 (1992).
7. Watabe, T., N. Ozawa, and A. Hiratsuka. Studies on metabolism and toxicity of styrene: VI. Regioselectivity in glutathione *S*-conjugation and hydrolysis of racemic, *R*- and *S*-phenyloxiranes in rat liver. *Biochem. Pharmacol.* **32**:777–785 (1983).
8. Bellucci, G., C. Chiappe, A. Cordoni, and F. Marioni. Substrate enantioselectivity in the rabbit liver microsomal epoxide hydrolase catalyzed hydrolysis of trans and cis 1-phenylpropene oxides: a comparison with styrene oxide. *Tetrahedron Asymmetry* **4**:1153–1160 (1993).
9. Armstrong, R. N., B. Kedzierski, W. Levin, and D. M. Jerina. Enantioselectivity of microsomal epoxide hydrolase toward arene oxide substrates. *J. Biol. Chem.* **256**:4726–4733 (1981).
10. Sayer, J. M., H. Yagi, P. J. van Bladeren, W. Levin, and D. M. Jerina. Stereoselectivity of microsomal epoxide hydrolase toward diol epoxides and tetrahydroepoxides derived from benz[a]anthracene. *J. Biol. Chem.* **260**:1630–1640 (1985).
11. Roberts-Thomson, S. J., M. E. McManus, R. H. Tukey, F. J. Gonzalez, and G. M. Holder. Polycyclic aza-aromatic carcinogens catalyzed by four expressed human cytochromes P450. *Cancer Res.* **55**:1052–1059 (1995).
12. Duke, C. C., and R. J. Wells. Investigation of readily available chiral compounds for preparative scale resolutions. *Aust. J. Chem.* **40**:1641–1654 (1987).
13. Boux, L. J., H. T. A. Cheung, G. M. Holder, and L. Moldovan. Potential metabolites of carcinogenic aza aromatic hydrocarbons synthesis of K-region oxide, phenol and dihydrodiols of 7-methylbenz[c]acridine. *Tetrahedron Lett.* **21**:2923–2926 (1980).
14. Duke, C. C., P. T. Murphy, and G. M. Holder. Synthesis of the non-K-region dihydrodiols of 7-methylbenz[c]acridine. *J. Org. Chem.* **49**:4446–4451 (1984).
15. Gill, J. H., A. M. Bonin, E. Podobna, R. S. U. Baker, C. C. Duke, C. A. Rosario, A. J. Ryan, and G. M. Holder. 7-Methylbenz[c]acridine: mutagenicity of some of its metabolites and derivatives, and the identification of *trans*-7-methylbenz[c]acridine-3,4-dihydrodiol as a microsomal metabolite. *Carcinogenesis* **7**:23–31 (1986).
16. Duke, C. C., and G. M. Holder. Endo-1,4,5,6,7,7-hexachlorobicyclo[2.2.1]-hept-5-ene-2-carboxylic acid, a superior resolving agent for the high performance liquid chromatographic separation of enantiomers of hydroxylated derivatives of two aza aromatic hydrocarbons. *J. Chromatogr.* **430**: 53–64 (1988).
17. Duke, C. C., T. W. Hambley, G. M. Holder, C. O. Navascues, S. J. Roberts-Thomson, and Y. Ye. Stereochemistry of the major rat liver microsomal metabolites of the carcinogen 7-methylbenz[c]acridine. *Chem. Res. Toxicol.* **4**:546–555 (1991).
18. McManus, M. E., W. M. Burgess, M. E. Veronese, A. Huggett, L. C. Quattrochi, and R. H. Tukey. Metabolism of 2-acetylaminofluorene and benzo[a]pyrene and the activation of food-derived heterocyclic amine mutagens by human cytochromes P-450. *Cancer Res.* **50**:3367–3376 (1990).
19. McManus, M. E., W. M. Burgess, E. G. Snyderwine, and I. Stupans. Specificity of rabbit cytochrome P-450 isozymes involved in the metabolic activation of the food derived mutagen 2-amino-3-methylimidazo[4,5-*f*]quinoline. *Cancer Res.* **48**:4513–4519 (1988).
20. Lowry, O. H., N. J. Rosebrough, A. L. Farr, and R. J. Randall. Protein measurement with the folin phenol reagent. *J. Biol. Chem.* **193**:265–275 (1951).
21. Skoda, R. C., A. Demierre, O. W. McBride, F. J. Gonzalez, and U. A. Meyer. Human microsomal xenobiotic epoxide hydrolase. *J. Biol. Chem.* **263**: 1549–1554 (1988).
22. Roberts-Thomson, S. J., M. E. McManus, R. H. Tukey, F. J. Gonzalez, and G. M. Holder. The catalytic activity of four expressed human cytochrome P450s towards benzo[a]pyrene and the isomers of its proximate carcinogen. *Biochem. Biophys. Res. Commun.* **192**:1373–1379 (1993).
23. Dansette, P., and D. M. Jerina. A facile synthesis of arene oxides at the K-regions of polycyclic hydrocarbons. *J. Am. Chem. Soc.* **96**:1224–1225 (1974).
24. Hassett, C., L. Aicher, J. S. Sidhu, and C. J. Omiecinski. Human microsomal epoxide hydrolase: genetic polymorphism and functional expression *in vitro* of amino acid variants. *Hum. Mol. Genet.* **3**:421–428 (1994).
25. Jackson, M. R., J. A. Craft, and B. Burchell. Nucleotide and deduced amino acid sequence of human liver microsomal epoxide hydrolase. *Nucleic Acids Res.* **15**:7188 (1987).
26. Westkaemper, R. B., and R. P. Hanzlik. Mechanistic studies of epoxide hydrolase utilizing a continuous spectrophotometric assay. *Arch. Biochem. Biophys.* **208**:195–204 (1981).
27. Dansette, P. M., V. B. Makedonska, and D. M. Jerina. Mechanism of catalysis for the hydration of substituted styrene oxides by hepatic epoxide hydrase. *Arch. Biochem. Biophys.* **187**:290–298 (1978).
28. Bellucci, G., C. Chiappe, L. Conti, F. Marioni, and G. Pierini. Substrate enantioselection in the microsomal epoxide hydrolase catalyzed hydrolysis of monosubstituted oxiranes: effect of branching of alkyl chains. *J. Org. Chem.* **54**:5978–5983 (1989).
29. Bellucci, G., C. Chiappe, A. Cordoni, and F. Marioni. The rabbit liver microsomal biotransformation of 1:1-dialkylethylenes: enantioface selection of epoxidation and enantioselectivity of epoxide hydrolysis. *Chirality* **6**:207–212 (1994).
30. Bellucci, G., G. Berti, M. Ferretti, E. Mastrorilli, and L. Silvestri. Enantioselectivity of the microsomal epoxide hydrolase catalyzed hydrolysis of *trans*-4,5-dimethyl-1,2-epoxycyclohexane. *J. Org. Chem.* **50**:1471–1474 (1985).
31. Levin, W., M. K. Buening, A. W. Wood, R. L. Chang, B. Kedzierski, D. R. Thakker, D. R. Boyd, G. S. Gadaginamath, R. N. Armstrong, H. Yagi, J. M. Karle, T. J. Slaga, D. M. Jerina, and A. H. Conney. An enantiomeric interaction in the metabolism and tumorigenicity of (+) and (−)-benzo[*a*]pyrene 7,8-oxide. *J. Biol. Chem.* **255**:9067–9074 (1980).
32. Mushtaq, M., H. B. Weems, and S. K. Yang. Stereoselective formation of enantiomeric K-region epoxide and *trans*-dihydrodiols in dibenz[*a*,*h*]anthracene metabolism. *Chem. Res. Toxicol.* **2**:84–93 (1989).
33. Weems, H. B., P. P. Fu, and S. K. Yang. Stereoselective metabolism of chrysene by rat liver microsomes: direct separation of diol enantiomers by chiral stationary phase h.p.l.c. *Carcinogenesis* **7**:1221–1230 (1986).
34. Haber, M. T., N. T. Nashed, and D. M. Jerina. Enantiomeric composition of *trans*-dihydrodiols formed from *meso*-K-region arene oxides by microsomal epoxide hydrolase. *Bioorg. & Med. Chem. Lett.* **2**:1729–1734 (1992).
35. Hassett, C., K. B. Robinson, N. B. Beck, and C. J. Omiecinski. The human microsomal epoxide hydrolase gene (EPHX1): complete nucleotide sequence and structural characterization. *Genomics* **23**:433–442 (1994).
36. Lacourciere, G. M., and R. N. Armstrong. Microsomal and soluble epoxide hydrolases are members of the same family of C-X bond hydrolase enzymes. *Chem. Res. Toxicol.* **7**:121–124 (1994).
37. Friedberg, T., B. Löllmann, R. Becker, R. Holler, and F. Oesch. The microsomal epoxide hydrolase has a single membrane signal anchor sequence which is dispensable for the catalytic activity of this protein. *Biochem. J.* **303**:967–972 (1994).
38. Beetham, J. K., D. Grant, M. Arand, J. Garbarino, T. Kiyosue, F. Pinot, F. Oesch, W. R. Belknap, K. Shinozaki, and B. D. Hammock. Gene evolution of epoxide hydrolases and recommended nomenclature. *DNA Cell Biol.* **14**:61–71 (1995).
39. Falany, C. N., P. McQuiddy, and C. B. Kasper. Structure and organization of the microsomal xenobiotic epoxide hydrolase gene. *J. Biol. Chem.* **262**: 5924–5930 (1987).
40. Bellucci, G., G. Berti, G. Ingrosso, and E. Mastrorilli. Stereoselectivity in the epoxide hydrase catalyzed hydrolysis of the stereoisomeric 4-tert-butyl-1:2-epoxycyclohexanes. *J. Org. Chem.* **45**:299–303 (1980).

Send reprint requests to: Dr. G. M. Holder, Department of Pharmacy, University of Sydney, N.S.W. 2006, Australia.